

Scientific paper

DFT Studies on η^6 -Coronene-Cr(CO)₃ Complexes

Lemi Türker* and Selçuk Gümüş

Middle East Technical University, Department of Chemistry, 06531, Ankara, Turkey

* Corresponding author: E-mail: lturker@metu.edu.tr
Phone: +90 312 2103244; fax: +90 312 2103200

Received: 11-07-2008

Abstract

Two types of Cr(CO)₃ complexes of coronene have been considered theoretically at the level of DFT (B3LYP/6-31G(d)), in order to investigate some molecular orbital, electronic and thermodynamic properties. The effect of complexation on the stability and aromaticity of coronene has been investigated by NICS calculations. According to the results, both in the gas phase and in aqueous solution, **B**-type complex has been found to be more stable than the **A**-type, however, the energy difference is such that **B** to **A** conversion could be possible by means of haptotropic shift of the chromium moiety. The interaction energy of the **B**-type complex is greater than the **A**-type, supporting the stability of the former over the latter. NICS calculations indicated that aromaticity of the outer rings has been drastically decreased by complexation.

Keywords: Coronene, Cr(CO)₃ complexes, haptotropic shift, NICS, aromaticity

1. Introduction

Coronene is a polycyclic aromatic hydrocarbon consisting of seven peri-fused rings.¹ It is a yellow material, which dissolves in solvents such as benzene, toluene, and dichloromethane. Its solutions give blue light fluorescence under UV light. Its emission spectrum is not symmetrical with its excitation spectrum and varies in the number of bands and their relative intensities with solvent. It has been used as a solvent probe, similarly to pyrene. The compound is of theoretical interest to organic chemists because of its aromaticity. It can be described by 20 resonance structures or by a set of three mobile Clar's sextets. In the latter case the most stable structure for coronene has only the three isolated outer sextets as fully aromatic although superaromaticity would still be possible when these sextets are able to migrate into the next ring.²

A wide range of η^6 -arene transition metal complexes are known. Of these, the arene-chromium tricarbonyl derivatives are perhaps the most studied ones.^{3–10} In general, the attachment of a metal tricarbonyl unit to an aromatic compound can have several consequences: 1) activation of the aromatic ring to nucleophilic attack; 2) enhancement of aryl-H acidities; 3) steric inhibition of attack on functional groups from the same side as the metal car-

bonyl group; 4) stabilization of any charge on carbons α and β to the arene-metal moiety.³ The first two of above mentioned effects stand for the most important ones. The attachment of Cr(CO)₃ groups to an aromatic ring leads to activation to attack by nucleophiles because the metal group acts as a kind of electron sink.

One of the first characteristics discovered in π -coordinated metal complexes, such as the tricarbonylchromium complex coordinated to polycyclic aromatic hydrocarbons (PAHs), was their ability to undergo thermal η^6, η^6 -inter-ring haptotropic rearrangements (IRHR) in which the π -coordinated metal migrates between different rings of the PAH.^{11–14} The simplest system where an IRHR takes place is in the (η^6 -naphthalene)-Cr(CO)₃ complex and their derivatives. For these species, mechanistic studies were performed to discern the nature of δ -coordinated metal binding.^{15–17} It was found that the interactions between low-lying unoccupied orbitals of Cr(CO)₃ and high-lying occupied π -orbitals of naphthalene represent the dominant bonding mechanism, the tricarbonylchromium acting in these complexes as a powerful electron withdrawing group.¹⁸ Moreover, some DFT calculations appeared in the literature very recently on Cr(CO)₃ complexes of polycyclic hydrocarbons (like naphthalene, phenanthrene perylene, chrysene).^{19–21}

2. Method

In the present study, after achieving the initial geometry optimizations by using MM2 method, followed by the semi-empirical PM3 self-consistent fields molecular orbital (SCF MO) method^{22,23} at the restricted level,^{24,25} then STO, RHF and Density Functional Theory (DFT-B3LYP)^{26,27} type quantum chemical calculations have been consecutively performed for the geometry optimizations with 6-31G(d) basis set to obtain energetically the most favorable structures of the presently considered species. The exchange term of B3LYP consists of hybrid Hartree-Fock and local spin density (LSD) exchange functions with Becke's gradient correlation to LSD exchange.^{27,28} The correlation term of B3LYP consists of Vosko, Wilk, Nusair (VWN3) local correlation functional²⁹ and Lee, Yang, Parr (LYP) correlation functional.³⁰

For each set of calculations, vibrational analyses were done (using the same basis set employed in the corresponding geometry optimizations). The normal mode analysis for each structure yielded no imaginary frequencies for the $3N-6$ vibrational degrees of freedom, where N is the number of atoms in the system. This indicates that the structure of each molecule corresponds at least to a local minimum on the potential energy surface. Furthermore, all the bond lengths were thoroughly searched in order to find out whether any bond cleavage occurred during the geometry optimization process. Geometry optimizations and the vibrational analysis computations were performed by using the Spartan 06 package program.³¹

For both of the complexes the interaction energies ($\Delta E = E_{\text{complex}} - E_{\text{coronene}} - E_{\text{Cr(CO)}_3} + E_{\text{BSSE}}$) and the stability of them in aqueous solution have also been calculated. Traditionally, self-consistent reaction field (SCRf) model was usually used to describe the effect of medium on chemical reactions. In this model, the microscopic information of molecular interaction between molecules and its surrounding molecules were neglected. Instead, the small water clusters were used to model solvent effects on some properties of the solute, such as tautomeric stabilities. Solvent effects were explored by using the SCRf method, and the polarizable continuum model (PCM) method was employed.³² Furthermore, the basis set superposition error (BSSE) analyses were carried out to correct the interaction energies with the counterpoise method, introduced by Boys and Bernardi.³³ The corresponding BSSE analyses were performed at the same theoretical levels.

Moreover, absolute NMR shielding values³⁴ were calculated using the Gauge-Independent Atomic Orbital method³⁵ with the restricted closed shell formalism employing 6-31G(d) basis set over B3LYP/6-31G(d) optimized geometries. NICS values were obtained by calculating absolute NMR shielding at the ring centers, NICS(0). NICS calculation have been done using Gaussian 03 package program.³⁶

3. Results and Discussion

In the present study, two types of Cr(CO)_3 complexes of coronene system are considered. The $\text{Cr(CO)}_3 \eta^6$ -complexes possess the Cr(CO)_3 tripod at two different positions of coronene system namely; **A**-type and **B**-type complexes (see Figure 1a).

Coronene, being a corannulene has some relevance to annulenes. Topologically, it has an inner periphery having six vertices (carbon atoms) and an outer periphery consisting of eighteen carbon atoms. Coronene is known as superaromatic because its inner and outer peripheries contain $4n+2$ atoms and that many π -electrons. Moreover, the Clar's sextet³⁷ spreads over the six benzenoid rings oriented around the core. However, complexation with certain transition metals, like the one presently considered, causes the π -electrons previously delocalized to be localized over the A- or B-type rings of coronene (Figure 1a).

In the case of **A**-type complex, 6 π -electrons are localized over the core region, thus the periphery becomes an aromatic annulene (see Figure 1, [18]-annulene). Whereas, in **B**-type complex, 6 π -electrons are localized in one of the peripheral benzenoid rings, thus the superaromaticity should be lost. However, two Clar's sextet could arise in the rest of the coronene system (see Figures 1b and 2). The embedded phenantrene system in **B**-type complex and [18]-annulene in **A**-type complex are the main substructures responsible for the aromaticity of these complexes. Thus, by complexation, corannulene should lose its superaromatic character. Whether a rapid haptotropic shift peripherally (isomerization)^{13,20} could occur in **B**-type complex to engender certain type of superaromatic character or not might be a matter of question.

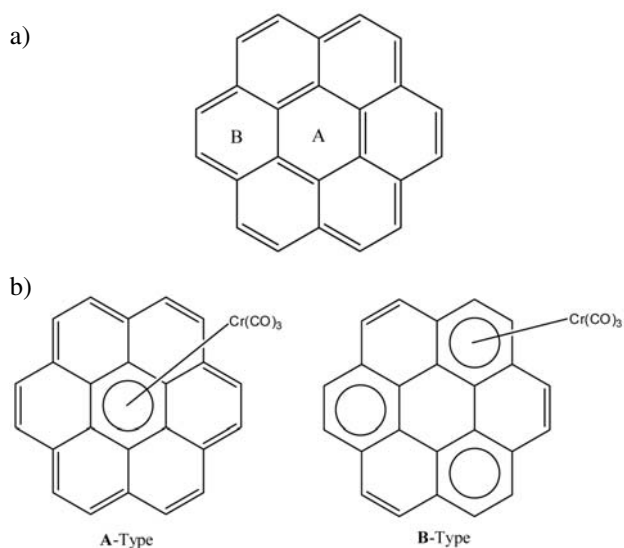


Figure 1. a) **A**- or **B**-type rings of coronene, b) Two Cr(CO)_3 coronene complexes.

3. 1. Bond Lengths

Figure 2 shows the bond lengths of the coronene complexes presently considered. The distance between the chromium atom and the center of the ring of complexation is 1.886 Å and 1.808 Å in **A**- and **B**-type complexes, respectively. In the **A**-type, the bond lengths of the central ring is almost constant (1.43 Å) whereas, the same ring in the **B**-type possesses bonds having lengths of 1.42–1.44 Å. In both complexes C–C bond length between the carbon atoms bearing a hydrogen atom is shorter than the other C–C bonds. In the case of **B**-type complex, bond lengths in the ring of complexation vary in the range of 1.39–1.44 Å. Whereas in the respective ring of **A**-type

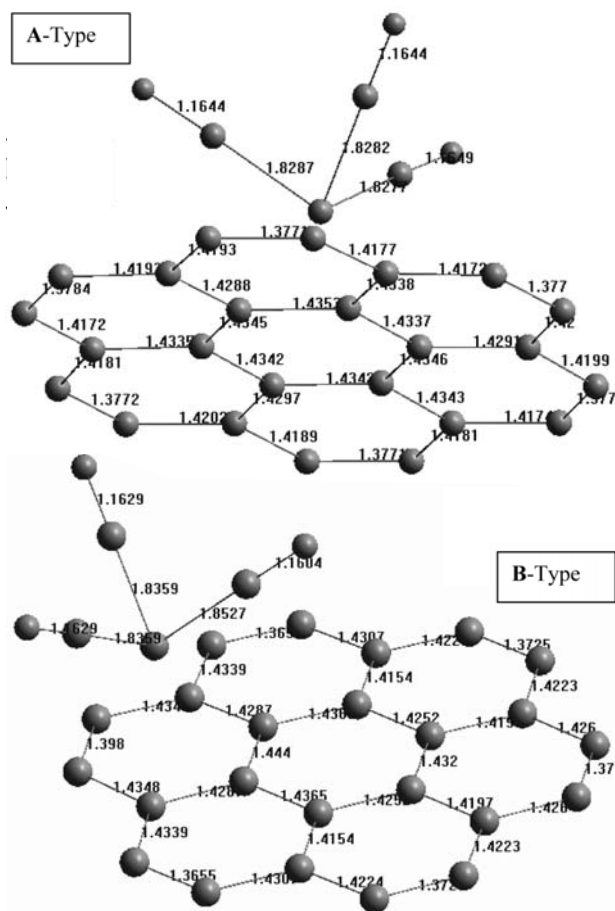


Figure 2. The bond lengths in **A**- and **B**-type complexes (in Å).

Table 1. Calculated energies and some thermodynamic properties of the coronene complexes. (Total energies are corrected with zero point energy).

	Total Energy ^a (Hartree)	Total Energy ^b (Hartree)	ZPE (kJ/mol)	Enthalpy* (kJ/mol)	Entropy (J/mol.K)	Entropy correction** (kJ/mol)	Cv (J/mol.K)
A -Type	-2306.0046	-2306.2200	804.1608	866.1659	655.9465	670.5955	388.5547
B -Type	-2306.0253	-2306.2411	805.0022	866.5163	657.7281	670.4146	388.0194

*Temp correction, **Hv-TSv, ^aTotal energy in gas phase, ^bTotal energy in aqueous solution

complex the bond lengths are more uniform (1.43 Å). The reason could be the higher symmetry of the **A**-type structure. In each case the sequence of bond lengths of the outer peripheral ring is such that two long (but not equal) bonds are followed by a short bond (HC–CH).

On the other hand, Cr–CO bond lengths are almost constant (1.82 Å) in the **A**-type complex whereas in the **B**-type the Cr–CO bond facing the bulk of the coronene surface is 1.85 Å which is longer than the other two bonds (1.83 Å).

3. 2. The Stabilities

3. 2. 1. Energetics

Table 1 shows the calculated total energies and some thermodynamic data together with the stability of the complexes in aqueous solution. According to the data, **B**-type complex has been found to be more stable both in the gas phase and in aqueous solution. The distances of the Cr from the aromatic plane in **A**- and **B**-type complexes are 1.886 Å and 1.808 Å, respectively, which may support the stability of the latter one. However, although **B**-type complex is more stable than the **A**-type, the energy difference is about 13 kcal and **B** to **A** conversion ($\Delta G^\circ = 13.2265$ kcal/mol), as long as the energy of the transition state is not very high could be possible by means of haptotropic shift of the chromium moiety.

The results of the interaction energy calculations in gas phase have been given in Table 2. All these calculations have been performed with B3LYP/6-31G(d) method. The interaction energies are negative values which mean that the complex systems are more stable than the reactants ($\Delta E = E_{\text{complex}} - E_{\text{coronene}} - E_{\text{Cr(CO)}_3} + E_{\text{BSSE}}$). Ac-

Table 2. DFT calculated energies of coronene, Cr(CO)₃, the BSSE energies and the interaction energies of the complexes (ΔE (A) and ΔE (B)).

	Energy (Hartree)	Energy (kcal/mol)
Coronene	-921.636772	
Cr(CO) ₃	-1384.324278	
BSSE (A)	0.022790134	
BSSE (B)	0.025127114	
ΔE (A)	-0.020759866	-13.02
ΔE (B)	-0.039122886	-24.54

According to the results given in Table 2, the interaction energy of the B-Type complex is greater than the A-Type, supporting the stability of the B-Type complex over the A-Type both in the gas phase and in the aqueous solution (see Table 1 for the stability in the gas phase and in the solution).

3. 2. 2. NICS

Aromaticity continues to be an actively investigated area of chemistry. The simplest criterion for aromatic compounds is that the presence of cyclic conjugated π -systems containing the proper number of π -electrons (i.e., the Hückel rule). While this criterion is robust enough to predict the aromaticity of a host of neutral and charged ring systems, it is not always a clear indicator of aromaticity for more complex systems (as in our case).

In the last few decades, extensive experimental and theoretical investigations have been carried out for cation/ π complexes involving aromatic rings to investigate the participation of these complexes in important processes related to chemical and biological recognition^{38–43}. Not only some transition metals or their complexes interact with π -electron cloud of aromatics, but tetramethylammonium like ions undergo interactions in solution with phenol⁴². Such an interaction has been investigated experimentally and supported by calculations in ref. 42.

Various probes of aromaticity are known in the literature such as para-delocalization index (PDI), the aromatic fluctuation index (FLU), the harmonic oscillator model of aromaticity index (HOMA) and nucleus-independent chemical shift (NICS)³⁸.

In 1996, Schleyer has introduced a simple and efficient probe for aromaticity: Nucleus-independent chemical shift (NICS),⁴⁴ which is the computed value of the negative magnetic shielding at some selected point in space, generally, at a ring or cage center. Negative NICS values denote aromaticity (–11.5 for benzene, –11.4 for naphthalene) and positive NICS values denote antiaromaticity (28.8 for cyclobutadiene) while small NICS values indicate non-aromaticity (–2.1 for cyclohexane, –1.1 for adamantane). NICS may be a useful indicator of aromaticity that usually correlates well with the other energetic, structural and magnetic criteria for aromaticity.^{34,45–48} Resonance energies and magnetic susceptibilities are measures of the overall aromaticity of a polycycle, but do not provide information about the individual rings. However, NICS is an effective probe for local aromaticity of individual rings of polycyclic systems.

In the present study, the effect of complexation on the aromaticity of the coronene system has been investigated via NICS calculations. NICS values at different ring centers have been calculated with B3LYP/6-31G(d) basis set over the fully optimized geometries. The geometry optimized structures of the coronene $\text{Cr}(\text{CO})_3$ complex systems considered here, as well as the coronene itself can be

seen in Figure 3. The arrows indicate the NICS values at the corresponding ring centers. Figure 4 shows the molecular electrostatic potential over coronene itself. The dark areas show the negative charge localizations. As seen from this figure the negative charge is mostly located on the corners but not across the bonds of the central ring. Indeed the bonds which are incident to the central ring are electron rich which make the outer rings have more aromatic character, as indicated by the NICS values. As a result, the outer rings are more likely to make π complexes (note that the tendency of the metal carbonyl group is to occupy a position where the electron density is maximum⁵⁰) with the electron deficient systems, in the present case with $\text{Cr}(\text{CO})_3$, which clearly explains the B-type complex being more favorable than the A-type.

As stated in the literature, six peripheral or outer 6-membered rings in coronene are diatropic with large negative NICS values, whereas the central 6-membered ring

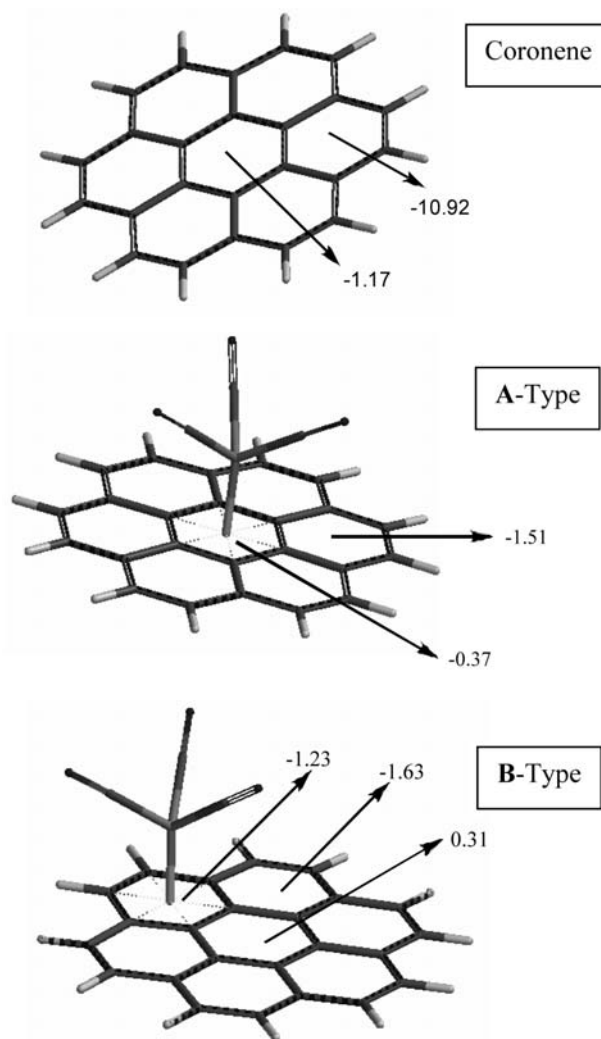


Figure 3. Geometry optimized structures of the coronene complexes (B3LYP/6-31G(d)). The arrows show the NICS values at the corresponding ring centers.

has a small positive⁵¹ or small negative NICS value.³⁸ According to the original interpretation of NICS,⁴⁴ the central ring must be essentially nonaromatic. Bühl stated that 6-membered rings surrounded by six other 6-membered rings, such as a central ring in coronene, are nonaromatic.⁵⁰ As can be seen from Figure 3, the NICS values calculated here are consistent with the literature results for the coronene structure. In order to investigate the effect of complexation on the aromaticity of the parent coronene, NICS values are calculated on different ring centers for the two Cr(CO)₃ coronene complexes. The results indicate that the aromaticity of the ring where the coordination of the metal takes place decreases by complexation. In fact, coordination of the metal to the central 6-membered ring of the parent coronene to form A-type complex system results a drastic decrease in the aromaticity of the outer 6-membered rings because the peripheral ring is just an annulenic system (superaromatic character of coronene is lost. Then, it is just [18]-annulene. However, according to the Hückel's rule it should be still aromatic). Güell et.al.³⁸ have observed a similar outcome with their calculations of aromaticity in the Li cation complex of coronene.



Figure 4. Molecular electrostatic potential over coronene itself. The darker areas show the greater negative charge localization.

3. 2. 3. The Frontier Molecular Orbital Energies

The frontier molecular orbital energies (HOMO and LUMO) as well as the interfrontier molecular orbital energy gap values ($\Delta\epsilon = \epsilon_{\text{LUMO}} - \epsilon_{\text{HOMO}}$) are shown in Table 3.

According to the data in Table 3, the complexation results in narrowing of the interfrontier energy gap. In

Table 3. Frontier molecular orbital energies and the interfrontier molecular orbital energy gap of the coronene and the two complex systems. (Energies are in eV).

	HOMO	LUMO	$\Delta\epsilon$
Coronene	-5.49	-1.32	4.17
A-Type	-4.86	-2.19	2.67
B-Type	-5.13	-1.99	3.14

A-type complex the extent of narrowing is more than the B-type complex even it has $\Delta\epsilon$ value smaller than coronene itself. Hence, the spectral (UV–VIS) characteristics of these complexes should arise in such a way that A-type complex absorbs at a longer whereas B-type complex at a shorter wavelength. The results show that both complexes have higher lying HOMOs and lower lying LUMOs than the parent coronene.

Figure 5 shows the HOMO and LUMO of the complexes obtained within the framework of B3LYP/6-31G(d) level of calculations. As seen there, in all the cases, the HOMO is mainly constructed by contribution of atomic orbitals around the complexation site. Whereas, the LUMO is generated by atomic orbitals of the coronene part. Thus, the coronene part of the complexes should be the main site of nucleophilic attack (even the LUMO energies for A- and B-type complexes are lower than the respective energy of coronene). However, no nucleophilic attack to coronene is mentioned in the literature but rarely some electrophilic attack has been reported such as the one with C₅₉N to form fullerene-coronene dyad.⁵²

The HOMO density of the complexes presently considered shows that the peripheral region has moderately high negative value. The region embedded in the bay of CO groups has the most positive value. Such a region, to a lesser extent exists also in between the other bay regions of the carbonyls. Physically those regions are very unlikely sites for electrophiles to attack whereas the peripheral zone is suitable for electrophilic attack.

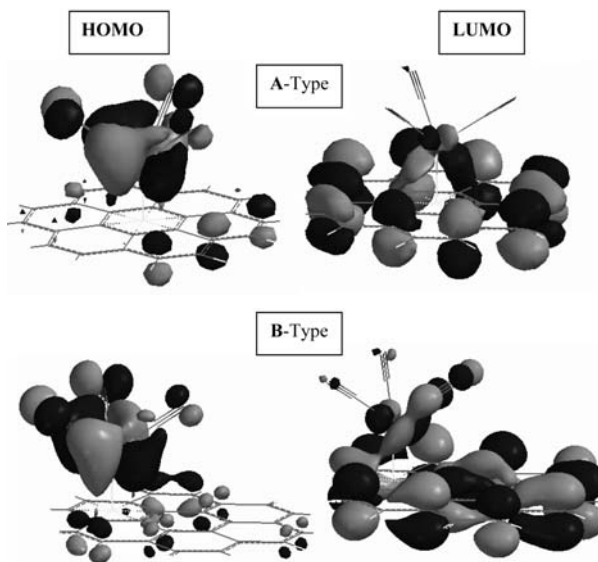


Figure 5. 3D HOMO and LUMO molecular orbital schemes of the A and B-type complexes.

On the other hand, the chemical potential (μ) which is equal to $-\chi_{\text{M}}$ (Mullikan's electro negativity) and η (absolute or chemical hardness) are important in reflecting chemical reactivity. The χ_{M} and η values are calculated

according to formulas given in ref. 53

$$\chi_M = (I+A)/2$$

$$\eta = (I-A)/2$$

where I and A are the ionization potential and electron affinity, respectively. Note that $I = -\epsilon_{\text{HOMO}}$ and $A = -\epsilon_{\text{LUMO}}$ within the validity of the Koopman's theorem.⁵⁴

When χ_M values are compared, B-type complex (3.56 eV) appears to be less susceptible to oxidations than the A-type (3.52 eV), as directly predicted from the respective HOMO energies. On the other hand, the LUMO energies are generally very dependent on the size of the basis set used and its quality. This means that the results for both χ_M and η can contain some errors.⁵³ Fortunately, relative values for a series of related molecules or a series of possible structures for a given molecule are often quite reliable.^{53,54} Therefore, χ_M and η values given here should be taken on relative basis rather than absolute values. Within this limitation, the η values predict that A-type complex (1.33 eV) is softer than the B-type (1.57 eV).

3. 3. Vibrational Spectra

The vibrational frequencies of the $\text{Cr}(\text{CO})_3$ coronene complexes are given in Figure 6 (at the DFT (B3LYP) level of theory using the standard 6-31G(d) basis set). The normal mode analysis for each structure yielded no imaginary frequencies for the 3N-6 vibrational degrees of freedom, where N is the number of atoms in the system. This indica-

tes that the structure of each molecule corresponds to at least a local minimum on the potential energy surface.

Generally, two spectra resemble each other, except with some intensity differences. The intense bands at 1990 and 2048 cm^{-1} for A-type and 2011 and 2057 cm^{-1} for B-type complex account for CO stretchings. These values are quite consistent with the literature data. Although, CO stretching energies differ from one complex to another with the effect of other ligands attached to the central metal atom, they are found to be around 1900–2100 cm^{-1} .^{55–57}

4. Conclusion

The DFT calculations presently carried out have revealed that yet nonexistent chromium tricarbonyl complexes of coronene should be stable species but endothermic in nature. The B-type complex is more favorable than the A-type, although the energy difference is small.

Metal carbonyls are known to have some catalytical effects as reported in the literature. Hence, the presently described coronene chromium tricarbonyl complexes might have some special usage because polyaromatic compounds, beside their some other interesting properties, are also known as capable of forming π -complexes with other aromatic compounds. Moreover, the A- and B-type complexes might have some stereo directive effect while they execute some catalytic activity. All these speculative points need further theoretical and experimental investigations to be tested for their validity.

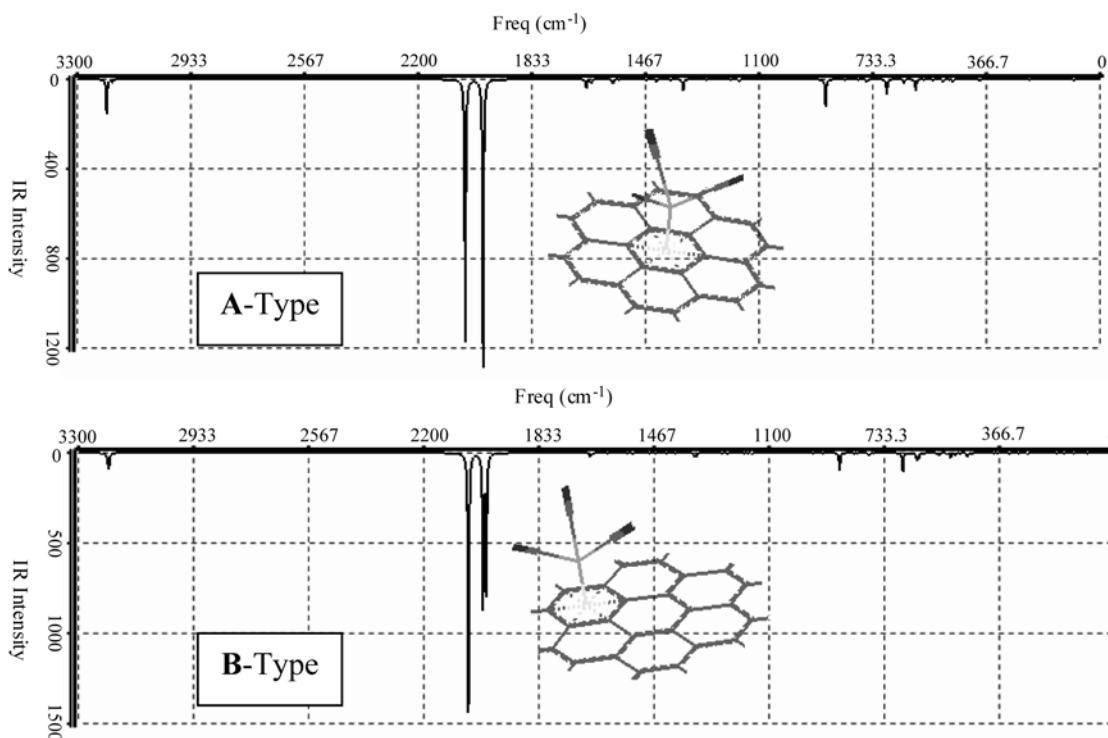


Figure 6. Calculated vibrational spectra of the two coronene complexes.

5. References

1. J. C. Fetzer: The Chemistry and Analysis of the Large Polycyclic Aromatic Hydrocarbons, Wiley, New York, **2000**.
2. <http://en.wikipedia.org/wiki/Coronene>
3. A. J. Pearson: Metallo-Organic Chemistry, Wiley, New York, **1985**.
4. B. C. Maity, V. M. Swamy, A. Sarkar, *Tetrahedron Lett.* **2001**, *42*, 4373–4376.
5. C. Bolm, K. Muñiz, *Chem. Soc. Rev.* **1999**, *28*, 51–60.
6. S. Sur, S. Ganesh, D. Pal, V. G. Puranik, P. Chakrabarti, A. Sarkar, *J. Org. Chem.* **1996**, *61*, 8362–8363.
7. S. K. Mandal, A. Sarkar, *J. Org. Chem.* **1999**, *64*, 2454–2458.
8. J. O. C. Jimenez-Halla, J. Robles, M. Sola, *J. Phys. Chem. A* **2008**, *112*, 1202–1213.
9. R. C. Dunbar, *J. Phys. Chem. A* **2002**, *106*, 9809–9819.
10. F. Nunzi, F. Mercuri, A. Sgamellotti, *J. Phys. Chem. B* **2002**, *106*, 10622–10633.
11. B. Deubzer, H. P. Fritz, C. G. Kreiter, K. Ofele, *J. Organomet. Chem.* **1967**, *7*, 289–299.
12. J. Muller, P. Gosser, M. Elian, *Angew. Chem. Int. Edit.* **1969**, *8*, 374–375.
13. K. H. Dötz, H. C. Jahr, *Chem. Rec.* **2004**, *4*, 61–71.
14. S. M. Hubig, S. V. Lindeman, J. K. Kochi, *Coord. Chem. Rev.* **2006**, *200–202*, 831–873.
15. T. A. Albright, P. Hofmann, R. Hoffmann, C. P. Lillya, P. A. Dobosh, *J. Am. Chem. Soc.* **1983**, *105*, 3396–3411.
16. K. H. Dötz, C. Stinner, M. Nieger, *J. Chem. Soc., Chem. Commun.* **1995**, 2535–2536.
17. R. U. Kirss, P. M. Treichel, *J. Am. Chem. Soc.* **1986**, *108*, 853–855.
18. C. A. Merlic, A. L. Zechman, M. M. Miller, *J. Am. Chem. Soc.* **2001**, *123*, 11101–11102.
19. A. Arrais, E. Diana, G. Gervasio, R. Gobetto, D. Marabello, P. L. Stanghellini, **2004**, 1505–1513.
20. S. Ketrat, S. Muller, M. Dolg, *J. Phys. Chem. A* **2007**, *111*, 6094–6102.
21. L. Türker, S. Gümüş, *Polycyclic Arom. Comp.* **2008**, *28*, 181–192.
22. J. J. P. Stewart, *J. Comput. Chem.* **1989**, *10*, 209–220.
23. J. J. P. Stewart, *J. Comput. Chem.* **1989**, *10*, 221–264.
24. A. R. Leach: Molecular Modeling, Longman, Essex, **1997**.
25. P. Fletcher: Practical Methods of Optimization, Wiley, New York, **1990**.
26. W. Kohn, L. J. Sham, *Phys. Rev.* **1965**, *140*, A1133–A1138.
27. R. G. Parr, W. Yang: Density Functional Theory of Atoms and Molecules, Oxford University Press, London, **1989**.
28. A. D. Becke, *Phys. Rev. A* **1988**, *38*, 3098–3100.
29. S. H. Vosko, L. Vilk, M. Nusair, *Can. J. Phys.* **1980**, *58*, 1200–1211.
30. C. Lee, W. Yang, R. G. Parr, *Phys. Rev. B* **1988**, *37*, 785–789.
31. Spartan 06 program, Wavefunction Inc., Irvine, CA 92612 USA.
32. C. Amovilli, V. Barone, R. Cammi, E. Cancès, M. Cossi, B. Mennucci, C. S. Pomelli, J. Tomasi, *Adv. Quantum Chem.* **1998**, *32*, 227.
33. S. F. Boys, F. Bernardi, *Mol. Phys.* **1970**, *19*, 553–566.
34. M. L. McKee in: G. R. Eaton, D. C. Wiley, O. Jardetzky (Eds.), ACS Symposium Series, No. 827, American Chemical Society, Washington DC, **2002**.
35. P. Pulay, J. F. Hinton, K. Wolinski, J. A. Tossel (Eds.), Nuclear Magnetic Shieldings and Molecular Structure, NATO ASI Series C, Kluwer, Netherlands, **1993**.
36. M. J. Frisch, G. W. Trucks, H. B. Schlegel, G. E. Scuseria, M. A. Robb, J. R. Cheeseman, J. A. Montgomery Jr., T. Vreven, K. N. Kudin, J. C. Burant, J. M. Millam, S. S. Iyengar, J. Tomasi, V. Barone, B. Mennucci, M. Cossi, G. Scalmani, N. Rega, G. A. Petersson, H. Nakatsuji, M. Hada, M. Ehara, K. Toyota, R. Fukuda, J. Hasegawa, M. Ishida, T. Nakajima, Y. Honda, O. Kitao, H. Nakai, M. Klene, X. Li, J. E. Knox, H. P. Hratchian, J. B. Cross, C. Adamo, J. Jaramillo, R. Gomperts, R. E. Stratmann, O. Yazyev, A. J. Austin, R. Cammi, C. Pomelli, J. W. Ochterski, P. Y. Ayala, K. Morokuma, G. A. Voth, P. Salvador, J. J. Dannenberg, V. G. Zakrzewski, S. Dapprich, A. D. Daniels, M. C. Strain, O. Farkas, D. K. Malick, A. D. Rabuck, K. Raghavachari, J. B. Foresman, J. V. Ortiz, Q. Cui, A. G. Baboul, S. Clifford, J. Cioslowski, B. B. Stefanov, G. Liu, A. Liashenko, P. Piskorz, I. Komaromi, R. L. Martin, D. J. Fox, T. Keith, M. A. Al-Laham, C. Y. Peng, A. Nanayakkara, M. Challacombe, P. M. W. Gill, B. Johnson, W. Chen, M. W. Wong, C. Gonzalez and J. A. Pople, Gaussian 03, Revision C. 02, Gaussian, Inc.: Wallingford CT, **2004**.
37. E. Clar: The Aromatic Sextet, Wiley, London, **1972**.
38. M. Guell, J. Poater, J. M. Luis, O. Mo, M. Yanez, M. Sola, *Chem. Phys. Chem.* **2005**, *6*, 2552–2561.
39. R. A. Kumpf, D. A. Dougherty, *Science* **1993**, *261*, 1708–1710.
40. J. C. Ma, D. A. Dougherty, *Chem. Rev.* **1997**, *97*, 1303–1324.
41. N. Zacharias, D. A. Dougherty, *Trends in Pharmacological Sciences*, **2002**, *23*, 281–287.
42. S. R. Lummis, D. L. Beene, N. J. Harrison, H. A. Lester, D. A. Dougherty, *Chemistry and Biology*, **2005**, *12*, 993–997.
43. M. Gaberscek, J. Mavri, *Chem. Phys. Lett.* **1999**, *308*, 421–427.
44. P. R. Schleyer, C. Maerker, A. Dransfeld, H. Jiao, N. J. R. E. Hommes, *J. Am. Chem. Soc.* **1996**, *118*, 6317–6318.
45. H. Jiao, P. R. Schleyer, *J. Phys. Org. Chem.* **1998**, *11*, 655–662.
46. P. R. Schleyer, B. Kiran, D. V. Simion, T. S. Sorensen, *J. Am. Chem. Soc.* **2000**, *122*, 510–513.
47. D. Quinonero, C. Garau, A. Frontera, P. Ballaster, A. Costa, P. M. Deya, *Chem. Eur. J.* **2002**, *8*, 433–438.
48. S. Patchkovskii, W. Thiel, *J. Mol. Model.* **2002**, *6*, 67–75.
49. O. A. Reutov: Advances in organometallic Chemistry, Mir Pub. Moscow, 1984.
50. M. Bühl, *Chem. Eur. J.* **1998**, *4*, 734–739.
51. G. Portella, J. Poater, M. Sola, *J. Phys. Org. Chem.* **2005**, *18*, 785–791.
52. F. Hauke, S. Atalick, D. M. Guldi, J. Mark, L. T. Scott, A. Hirsch, *Chem. Comm.* **2004**, 766–767.
53. R. G. Pearson: Chemical Hardness, Wiley-VCH, New York, **1997**.

54. C. J. Cramer: Essentials of Computational Chemistry, Wiley, Sussex, 2004.
55. L. Andrews, M. Zhou, G. L. Gutsev, X. Wang, *J. Phys. Chem. A* 2003, 107, 561–569.
56. S. Özkar, C. Kayran, N. Demir, *J. Organometallic Chem.* 2003, 688, 62–67.
57. F. Kozanoglu, S. Saldamlı, S. Özkar, *J. Organometallic Chem.* 2002, 658, 274–280.

Povzetek

Dva tipa kompleksov $\text{Cr}(\text{CO})_3$ s koronenom smo študirali z DFT metodo na nivoju B3LYP/6-31G(d). Zanimale so nas elektronske in termodinamske lastnosti. Efekt kompleksacije na aromatičnost in stabilnost smo študirali z NICS (Nucleus Independent Chemical Shift) metodo. Kompleks **B** je bolj stabilen v vodni raztopini in plinski fazi kot kompleks **A**. Energijska razlika dopušča interkonverzijo s haptotropskim premikom kromove skupine. Interakcijska energija za kompleks **B** je bolj ugodna kot za **A**. NICS izračuni kažejo, da se zunanjim aromatskim obročem pri kompleksaciji znižata aromatičnost.